HOKKAIDO UNIVERSITY

Title	Role of His63 in HutZ from Vibrio cholerae in the heme degradation reaction and heme binding
Author(s)	Uchida, Takeshi; Dojun, Nobuhiko; Sekine, Yukari et al.
Citation	Dalton Transactions, 48(16), 5408-5416 https://doi.org/10.1039/C9DT00926D
Issue Date	2019-04-28
Doc URL	https://hdl.handle.net/2115/77738
Type	journal article
File Information	DALTON T48-16_5408-5416.pdf

Hokkaido University Collection of Scholarly and Academic Papers : HUSCAP

Please do not adjust margins

Journal Name

ARTICLE

Role of His63 in HutZ from *Vibrio cholerae* in the heme degradation reaction and heme binding

Received 00th January 20xx,
Accepted 00th January 20xx

DOI: 10.1039/x0xx00000x

www.rsc.org/

Takeshi Uchida,*[a,b] Nobuhiko Dojun,[b] Yukari Sekine,[b] and Koichiro Ishimori[a,b]

HutZ from *Vibrio cholerae* is a dimeric enzyme that catalyzes oxygen-dependent degradation of heme via a similar catalytic mechanism to mammalian heme oxygenase. However, HutZ oxidizes the β- or δ-meso position of heme at a ~1:1 ratio distinct from heme oxygenase, which initiates the degradation of heme solely at the α-meso position. His63 is a residue that potentially forms hydrogen bond with the heme 7-propionate group. To establish the role of His63 in regioselectivity of heme degradation by HutZ and heme binding, we constructed mutants of His63. Interestingly, the H63L mutant retained a comparable level of β- or δ-regioselectivity as wild-type HutZ. Ascorbic acid-assisted heme degradation by HutZ is pH-dependent, showing activity at pH 6.0 but not above pH 8.0. Compared to the wild-type protein, the H63L mutant was inactive, even at pH 6.0, and affinity for heme was significantly decreased in contrast with a comparable heme binding affinity at pH 8.0, as observed for the mutant of Asp132 to Val, which is located within hydrogen bonding distance of the heme axial ligand His170, but in a different protomer. In addition, the distance between heme and Trp109 increased from 16-18 Å for wild-type HutZ to 24-28 Å for the H63L mutant, indicating that protomer orientation is altered by the mutation, since Trp109 is in another subunit of the heme axial ligand. Our results collectively suggest that His63 positioned near heme does not contribute to regioselectivity of heme degradation but plays a key role in maintaining the orientation of subunits for HutZ to function of heme degradation.

1. Introduction

Iron is an essential element for growth and survival for most bacteria that serves as a cofactor in key metabolic processes, such as electron transfer and energy transduction. Bacteria have evolved sophisticated iron acquisition systems owing to the limited availability of iron under normal growth conditions.[1] For instance, a number of bacteria synthesize and secrete low molecular weight compounds known as siderophores, which bind ferric iron with high affinity from several sources, such as soil, water and transferrin.[2–5] Iron-bound siderophores are taken up through receptor proteins in the outer membrane.[6]

The majority of pathogens additionally utilize siderophore-independent iron uptake systems, whereby heme (iron-protoporphyrin IX) is a common iron source. Heme receptor proteins in the outer membrane accept heme either directly or from hemoglobin and transfer it into the cell periplasm. Periplasmic heme-binding proteins carry heme to the inner membrane receptors, which transfer heme into the cytoplasm across the inner membrane. In the cytoplasm, the porphyrin ring is degraded in an oxygen-dependent manner to release the iron atom.[7,8] The gram-negative bacterium, *Vibrio cholerae*, is the causative agent of cholera. Based on the genome sequence of *V. cholerae* and bioinformatics-based predictions, putative genes encoding heme acquisition have been identified, termed *hut* (heme utilization).[9–11] Members of the Hut family include membrane heme transport proteins (HutA, HutC, HutD and HutR) and heme carrier proteins (HutB and HutX).[12,13] Heme is degraded to release iron by HutZ, which exists in the periplasm. A previous study by our group established that HutZ possesses heme degradation activity,[14] although it is proposed as a heme storage and not heme oxygenase (HO) protein.[15] HutZ, a dimeric protein, can cleave heme to biliverdin via verdoheme, similar to mammalian HOs.[14] However, the cleavage site of the porphyrin ring is β- or δ-[14] and not α-meso carbon as reported for HOs.[16] This differential regioselectivity indicates different heme degradation mechanisms of HutZ from those of well-characterized HOs.

Although the crystal structure of the heme-HutZ complex has not been established to date, that of a homologous protein, HugZ from *Helicobacter pylori*, is available.[17] Examination of the HugZ structure drew our attention to the presence of a hydrogen bond around the heme. His63 (numbering for HutZ) is located close to heme 7-propionate, (Fig. 1, Fig. S1†). In human HO-1, heme propionate acid interacts with highly conserved Arg183 and Tyr134.[18,19] Mutational analyses further revealed that Arg183 is one of the

[a] Department of Chemistry, Faculty of Science, Hokkaido University, Sapporo 060-0810, Japan. E-mail: uchida@sci.hokudai.ac.jp
[b] Graduate School of Chemical Sciences and Engineering, Hokkaido University, Sapporo 060-8628, Japan

†Electronic Supplementary Information (ESI) available: [details of any supplementary information available should be included here]. See DOI: 10.1039/x0xx00000x

Please do not adjust margins

Please do not adjust margins

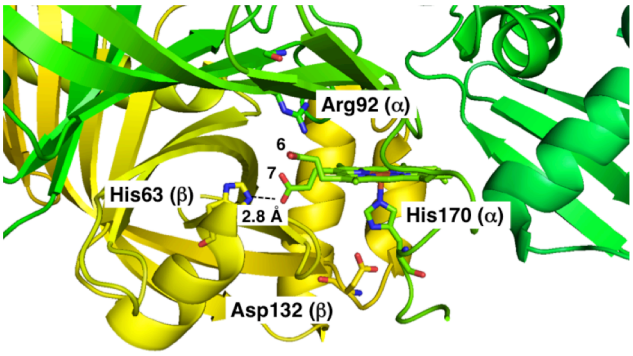


Fig. 1 Crystal structure of HugZ from *Helicobacter pylori* (PDB ID code 3GAS). Residues involved in the heme degradation reaction of HutZ are shown. Amino acid residues are numbered according to the sequence of HutZ from *V. cholerae*. α and β indicate the subunits. The number 6 and 7 shows the position of the propionate groups. The nearest distances between His63 and propionate 7 is estimated to be 2.8 Å.

factors determining the regioselectivity of heme degradation.[20] The heme macrocycle is cleaved at α-meso carbon to produce α-biliverdin by wild-type (WT) HO-1.[16] An earlier study reported that mutation of Arg183 to Glu leads to loss of α-regioselectivity and production of three biliverdin isomers (α, β, and δ) in the reaction with ascorbic acid.[20] This interaction is conserved in HO from *Pseudomonas aeruginosa* (*pa*-HO). In *pa*-HO, Lys34 and Lys132 interact with 6-propionate of heme with β- (28%) and δ-regioselectivity (72%).[21] Disruption of these interactions by substitution of the above amino acids with Ala led to increased α-regioselectivity (18%) to compensate for δ-regioselectivity.[21,22]

The *pa*-HO structure shares a homologous fold with HO-1.[18,23] In the heme-HO-1 complex, Lys18 and Tyr134 interact with 7-propionate of heme[18,19] and HO-1 degrades heme with complete α-regioselectivity.[16] The corresponding residues of *pa*-HO are Asn19 and Phe117, which do not interact with the heme propionate. The heme of *pa*-HO is rotated in-plane ~110°, compared with HO-1, which leads to cleavage at the δ-meso carbon.[24] Introduction of interactions with propionate by replacing Asn19 and Phe117 with Lys and Tyr, respectively, generated the two conformers with the different heme seats, one the same as that in WT *pa*-HO with δ-regioselectivity and the other the same as that in WT HO-1 with α-regioselectivity.[21] These findings suggest that hydrogen bonding with heme propionates is a potential key factor in controlling the regioselectivity of heme degradation.

Recently, new kinds of heme degrading enzyme named IsdG and MhuD were found from bacteria and also lower eukaryotes.[25–27] IsdG and MhuD are structurally different from canonical HO and their final product of heme is not biliverdin, but staphylobilin and mycobilin, respectively. MhuD cleaves a tetrapyrrole ring at a position with retention of the α-meso carbon as an aldehyde and further oxygenation at either the β- or δ-meso position. The propionate groups of MhuD from *Mycobacterium tuberculosis* interact with Arg22 and Arg26.[28] Although the mutation of Arg22 did not cause any effect on the enzymatic products, mutation of Arg26 changed the product from mycobilin to biliverdin, indicating that the interaction between Arg26 and heme propionate plays a key role in the heme degradation reaction of MhuD.[29]

In this study, we replaced His63, which is presumably located within the hydrogen bonding distance of 7-propionate, whose the nearest distance to His63 was estimated to be 2.8 Å on the basis of the crystal structure of HugZ (Fig. 1)[17], with Leu to gain insights into the role of His63 in determining regioselectivity of heme degradation by HutZ and heme binding. The H63L mutant did not affect regioselectivity, distinct from the results obtained with human HO mutants. Notably, however, mutation of His63 resulted in loss of pH-dependent heme degradation activity. WT HutZ is active in ascorbic acid-assisted heme degradation at pH 6.0 but inactive at pH >8.0.[14] The H63L mutant was inactive at even pH 6.0. Furthermore, although a mutational and docking study proposed coordination of His63 to heme,[30] the mutation of His63 to Leu did not affect the absorption spectrum and affinity for heme at pH 8.0. However, the affinity of the H63L mutant for heme at pH 6.0 was markedly decreased. Fluorescence spectral data suggested an elongated distance between heme and Trp109 in the mutant, indicating changes in interactions at the dimer interface. These findings indicate that His63 does not contribute to regioselectivity of heme degradation but participates in fixing subunit-subunit interactions essential for HutZ to bind heme and function as a heme-degrading enzyme.

2. Materials and methods

Materials

The chemicals used in this study were purchased from Wako Pure Chemical Industries (Osaka, Japan), Nacalai Tesque (Kyoto, Japan) or Sigma-Aldrich (St. Louis, MO, USA), and used without further purification.

Expression and purification of HutZ

Expression and purification of HutZ mutants were conducted as described previously.[14,31] Briefly, the HutZ plasmid with a His_6 tag was expressed in *Escherichia coli* BL21(DE3) cells. The protein was isolated via a HisTrap HP column (GE Healthcare, Uppsala, Sweden), followed by a gel filtration column (HiLoad 16/60 Superdex 200 pg, GE Healthcare) equilibrated with 50 mM Tris-HCl and 150 mM NaCl (pH 8.0). Purity was confirmed as > 90% via SDS-PAGE. The protein concentrations of heme-unbound and heme-bound HutZ were determined by absorbance at 280 nm with a molar extinction coefficient (ε_{280}) obtained using ProtParam server (http://web.expasy.org/protparam/) of 9.97 $mM^{-1}cm^{-1}$ and 412 nm with ε_{412} of 170 $mM^{-1}cm^{-1}$.[15]

Mutagenesis was conducted with the aid of the PrimeSTAR mutagenesis basal kit from Takara Bio (Otsu, Japan) using wild-type expression vector as the template. DNA oligonucleotides were purchased from Eurofins Genomics Inc (Tokyo, Japan). Genes were confirmed via sequencing (Eurofins Genomics Inc.) to ensure that only the desired mutations were introduced.

This journal is © The Royal Society of Chemistry 20xx

Please do not adjust margins

Please do not adjust margins

Spectroscopy

Optical spectra of purified proteins were recorded with a UV-visible spectrophotometer (V-660, Jasco, Tokyo, Japan) at 25 °C. Resonance Raman spectra were obtained with a single monochromator (SPEX500M, Jobin Yvon, NJ, USA) equipped with a liquid nitrogen-cooled CCD detector (Spec-10:400B/LN, Roper Scientific, Princeton, NJ, USA). The excitation wavelengths employed were 413.1 and 441.6 nm from a krypton ion (BeamLok 2060, Spectra Physics, CA, USA) and helium-cadmium (IK5651R, Kimmon Koha, Tokyo, Japan) lasers, respectively. Laser power at the sample point was adjusted to ~5 mW for the ferric and ferrous forms and 0.1 mW for the CO-bound form to prevent photodissociation. Raman shifts were calibrated with indene, CCl_4, acetone, and an aqueous solution of ferrocyanide. The accuracy of the peak positions of well-defined Raman bands was ±1 cm^{-1}. Sample concentrations for resonance Raman experiments were ~10 μM in 50 mM Tris-HCl and 150 mM NaCl (pH 8.0).

Fluorescence spectra were recorded using a FP-8500 spectrometer (Jasco). Protein samples were excited at 295 nm to avoid contribution from tyrosine residues. The HutZ concentration in samples was 3 μM in 50 mM Tris-HCl and 150 mM NaCl (pH 8.0). The distance (r) between tryptophan and heme was estimated from the efficiency (E) of Förster energy transfer from tryptophan to heme, defined as:

$$E = \frac{R_0^6}{R_0^6 + r^6} \quad (1)$$

where R_0 represents the Förster distance and R_0 for heme and tryptophan is 29 Å.[32] The energy transfer efficiency, E, was calculated using the fluorescence intensity of apo-HutZ (F_{apo}) and heme-HutZ (F_{heme}):

$$E = \frac{F_{apo} - F_{heme}}{F_{apo}} \quad (2)$$

The spectra were recorded in either 50 mM MES (pH 6.0–6.6), HEPES (pH 6.8–7.6) or Tris buffer (pH 7.8–8.8) containing 150 mM NaCl.

HPLC Analysis of Biliverdin Isomers

Heme degradation was performed by adding 0.1 mM H_2O_2 to a solution of heme-HutZ (5 μM) in 50 mM Tris-HCl and 150 mM NaCl (pH 8.0). The solution was incubated for 30 min at room temperature, followed by the addition of 1 mM ascorbic acid. The reactant was purified using a Supelclean LC-18 solid phase extraction column (Sigma-Aldrich). To extract biliverdin products, a few drops of 1 M hydrochloric acid were added before extraction of the reaction mixture with methanol.

The biliverdin products were analyzed on a HPLC system (LC-2000, Jasco) equipped with a ZORBAX Extend-C18 column (3.0 × 150 mm, 3.5 μm; Agilent Technologies, Santa Clara, CA, USA). Solvents A and B were 10 mM ammonium acetate and methanol, respectively. The running conditions were as follows: flow rate, 1.0 mL min^{-1}; 30% B for 5 min, 30-70% B in 0.1 min, 70-95% B in 25 min, 95% B for 7 min, 95-30% B in 1 min, and 30% B for 20 min. The eluent was monitored at 375 nm. The standards of the biliverdin dimethyl esters were prepared as published elsewhere.[33]

Heme Degradation Activity

The heme degradation reaction of HutZ was monitored spectrophotometrically. Briefly, 1,900 μL hemin-reconstituted protein solution (final concentration, 10 μM) in 50 mM Tris-HCl and 150 mM NaCl (pH 8.0) was placed in a cuvette. The reaction was initiated by the addition of 100 μL of 4 mM H_2O_2 or 20 mM ascorbic acid in the same buffer at 25 °C. Spectra were recorded at intervals of 1 min over 10 min for H_2O_2 and 2 min over 30 min for ascorbic acid. For reaction with ascorbic acid (final concentration of 1 mM), 1 mg mL^{-1} bovine liver catalase was added to suppress H_2O_2. After the reaction, ferrozine (Dojindo, Kumamoto, Japan) was added to a final concentration of 1 mM. The amount of iron released was calculated based on absorbance at 562 nm (ε_{562} = 29 $mM^{-1}cm^{-1}$).

Affinity of HutZ for Heme

Heme binding was monitored based on difference spectroscopy in the Soret region of the UV-visible absorption spectrum. Hemin was dissolved in 0.1 M NaOH, and its concentration was determined on the basis of absorbance at 385 nm using an extinction coefficient (ε_{385}) of 58.44 mM^{-1} cm^{-1}.[34] Successive aliquots of 0.5 mM hemin were added to both the sample cuvette containing 10 μM HutZ in 50 mM Tris-HCL and 150 mM NaCl (pH 8.0) and reference cuvette. No pH change in the medium was observed after the addition of the hemin solution. Spectra were recorded 3 min after the addition of each heme aliquot. The absorbance difference at 412 nm was plotted as a function of heme concentration and apparent dissociation constant ($K_{d,heme}$) calculated using a quadratic binding equation:

$$\Delta A = \Delta A_{max} \frac{[P] + [H] + K_{d,heme} - \sqrt{([P] + [H] + K_{d,heme})^2 - 4[P][H]}}{2[P]} \quad (3)$$

where [P] and [H] represent total protein and hemin concentrations, respectively.

Cyanide Binding

The cyanide binding rate was measured by monitoring the decrease in absorbance at 412 nm using a stopped-flow apparatus (Unisoku, Osaka, Japan). In a typical cyanide binding experiment, one syringe contained 3 μM HutZ (50 mM Tris-HCl and 150 mM NaCl, pH 8.0) and another contained at least 100-fold excess of cyanide. Three determinations were performed for each ligand concentration. The mean of the pseudo-first-order rate constant, k_{obs}, was used to calculate the second-order rate constants obtained from the slope of a plot of k_{obs} versus ligand concentration ($k_{obs} = k_{on}[CN] + k_{off}$).

3. Results and discussion

Resonance Raman Spectra of the Heme-H63L Mutant

Please do not adjust margins

Please do not adjust margins

The hydrogen bonding status of the peripheral groups of HutZ-bound heme was examined via resonance Raman spectroscopy, since the frequency of the propionate bending mode, $\delta(C\beta\text{-}C_c\text{-}C_d)$, usually observed at 360–380 cm^{-1},[35,36] is associated with the strength of hydrogen bonding to the propionate groups and undergoes a downshift upon weakening of hydrogen bonding.[37]

Overall, the resonance Raman spectra of the heme-H63L mutant in all three bound forms (ferric, ferrous and CO) were almost identical to the corresponding spectra of heme-WT HutZ (Fig. 2), clearly indicating that replacement of His63 induces no structural changes around the heme.

Insensitivity of the $\delta(C\beta\text{-}C_c\text{-}C_d)$ mode to mutation was additionally observed in the heme axial ligand mutant of HutZ. His170 is predicated as a putative heme ligand of HutZ based on comparison of its amino acid sequence to that of HugZ from *H. pylori*.[17] However, an earlier study has shown that a His170 mutant (H170A) can still bind heme.[31] Considering that double mutation of His170 and His63 results in loss of heme binding ability and His63 is the sole His in the heme-binding pocket apart from His170 (Fig. 1),[17,31] heme is expected to bind to His63 in the H170A mutant. Thus, the hydrogen bonding status of the heme peripheral group in the H170A mutant should be distinct from that of WT HutZ. However, the frequencies of $\delta(C\beta\text{-}C_c\text{-}C_d)$ for the H170A mutant were almost identical to those of heme-WT HutZ,[31] indicating that the frequency of the propionate group of heme in HutZ might be insensitive to hydrogen bond formation.

A broad band at 414 cm^{-1} for ferrous heme-WT HutZ is assigned to the vinyl bending mode, $\delta(C\beta\text{-}C_a\text{-}C_b)$, compared with myoglobin.[36] This band was split into two bands at 407 and 427 cm^{-1} in the spectrum of the ferrous heme-H63L mutant (Fig. 2B). The frequency of this mode for ferric and CO-bound heme-H63L mutant forms was also slightly shifted (Fig. 2A, C). Thus, although cleavage of the hydrogen bond to propionate groups was not confirmed, the structure around heme vinyl groups was clearly perturbed by the His63 mutation.

The His-bound five-coordinate high-spin heme facilitates detection of Fe-His stretching modes ($\nu_{Fe\text{-}His}$) at around 200-250 cm^{-1}.[38] Therefore, we observed the $\nu_{Fe\text{-}His}$ mode of the heme-H63L mutant. The resonance Raman spectrum of the ferrous heme-H63L mutant excited at 441.6 nm exhibited a prominent band at 227 cm^{-1}. The frequency of this band was identical to that of $\nu_{Fe\text{-}His}$ of heme-WT HutZ (Fig. 2B)[14], implying that replacement of His63 with Leu does not alter the structure at the proximal side of heme.

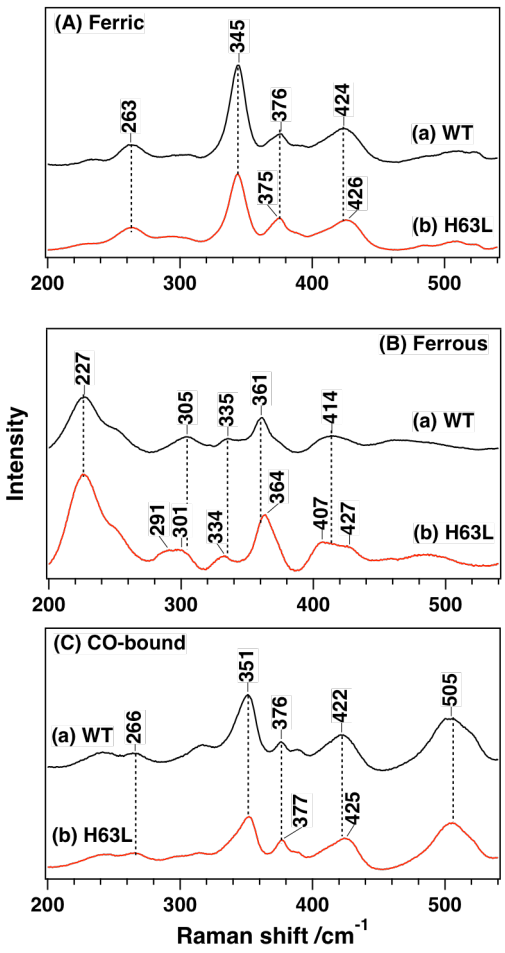


Fig. 2 Resonance Raman spectra of heme-HutZ. Resonance Raman spectra of ferric (A), ferrous (B), and CO-bound (C) forms of heme-WT and H63L mutant HutZ. The protein concentration was 10 μM in 50 mM Tris-HCl, 150 mM NaCl (pH 8.0). The excitation wavelength for the ferric and CO-bound forms was 413.1 nm and that for the ferrous form was 441.6 nm.

Determinants of the Regioselectivity of Heme Degradation by HutZ

The regioselectivity of heme degradation by the H63L mutant was analyzed using HPLC. The reaction was conducted at pH 6.0 using ascorbic acid as an electron source. In the reaction of hemin, four products were observed at 14.8 (biliverdin IXα), 20.5 (biliverdin IXβ), 22.7 (biliverdin IXδ), and 31.9 min (biliverdin IXγ) (Fig. 3). Peaks were assigned on the basis of a previous report.[39] In the chromatogram of the H63L mutant, two large peaks appeared. The main products of the H63L mutant were biliverdin IXβ (t = 20.7 min) and biliverdin IXδ (t = 22.9 min), similar to WT HutZ. The appearance of tiny amounts of biliverdin IXα (t = 14.9 min) and small increase in the biliverdin IXδ may be attributed to perturbation of hydrogen bonding to the heme propionates in this mutant, but the effects were modest.

One possibility is that insertion of Leu in the H63L mutant sterically hinders heme rotation in the heme-binding pocket, which leads to retention of the regioselectivity of heme breakage. To examine this theory, His63 was replaced with Gly to increase the space for heme rotation. The regioselectivity of heme degradation of the H63G mutant was analogous to that of WT HutZ (Fig. S2†). If heme is able to rotate freely, regioselectivity is lost and cleavage should occur on every four sites (α, β, γ, and δ). Retention of β- and δ-regioselectivity by the heme-H63G mutant suggests that free rotation of heme does not occur, and thus heme sits in the appropriate position for degradation, even when His63 is replaced with Gly.

This journal is © The Royal Society of Chemistry 20xx

Please do not adjust margins

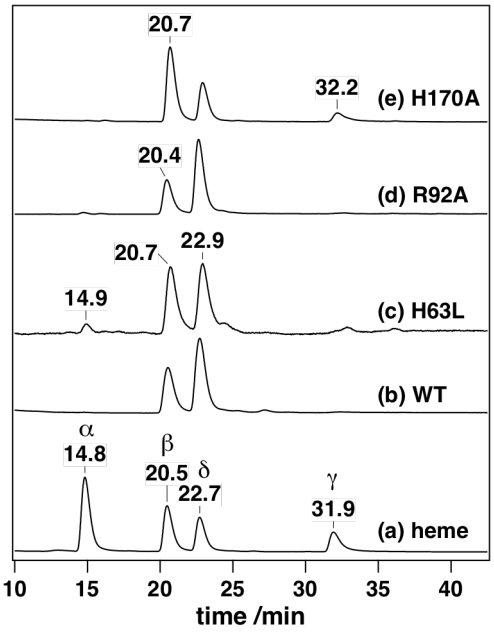


Fig. 3 Regiospecificity of heme degradation by HutZ. HPLC chromatography of products from reaction of free heme (a), heme-WT (b), heme-H63L mutant (c), heme-R92A mutant (d) and heme-H170A mutant (e) in 50 mM Tris-HCl and 150 mM NaCl with 0.1 mM H_2O_2 and 1 mM ascorbic acid.

In mammalian HO-1, four residues (Arg183, Lys18, Lys179, and Tyr134) generate hydrogen bonds with the heme propionates.[18] Upon mutation of Arg183 to Glu, the ratio of biliverdin IXα was decreased from 100 to 79%, along with an increase in biliverdin IXδ from 0 to 19%, suggesting that hydrogen bonding to heme propionate is crucial in controlling the regioselectivity of heme degradation in HO-1.[33] Here, we constructed two HutZ mutants to investigate whether hydrogen bonding to heme propionates plays a role in determining the regiospecificity of heme degradation. Although His63 of HutZ were expected to be located within the hydrogen bonding distance of the heme propionates on the basis of the crystal structure of HugZ from *H. pylori* (Fig. 1),[17] the effects of mutation of His63 were insignificant, compared with results obtained for HO mutants in which the hydrogen bonds between heme propionates and amino acid residues were disrupted. These results suggest that His63 is unlikely to be essential to determine the regioselectivity of heme degradation for HutZ, although it is uncertain that His63 forms hydrogen bond with heme propionate.

Since His63 did not contribute to the regioselectivity of heme degradation, we focused our attention on other residues in the heme binding site. Arg92 is a possible determinant of regioselectivity, since it is assumed to interact with the iron-bound ligand (Fig. S3†).[17] The chromatogram of reaction products of the R92A mutant was slightly different from that of WT HutZ, whereby the intensity of the band at 22.7 min was about twice as large as that at 20.4 min (Fig. 3), indicating that the R92A prefers biliverdin IXδ to biliverdin IXβ.

The heme axial ligand, His170, was further replaced with Ala. In this mutant, the band from biliverdin IXβ at 20.7 min was enhanced at the expense of the band from biliverdin IXδ at 22.9 min (Fig. 3). In addition, a new small band appeared at 32.2 min corresponding to biliverdin IXγ. However, the effects of mutation at Arg92 and His170 were relatively modest. In view of these results, we suggest that the regioselectivity of heme degradation of HutZ is not determined by specific interactions such as propionate groups while the environment of the heme binding site itself appears to be an important determinant.

Heme Degradation Reaction of the H63L Mutant

The heme degradation reaction of the heme-H63L mutant was measured using H_2O_2 (Fig. 4C). The rapid decrease in the Soret band with a concomitant increase in absorbance at 650 nm suggested the formation of verdoheme, similar to that observed for heme-WT HutZ.[14] At 3 min after the addition of H_2O_2, absorbance of the Soret band at 411 nm for the heme-H63L mutant was ~45% of the initial height, compared to ~60% for heme-WT HutZ.[14] The rate constant of absorption changes at the Soret maximum for heme-H63L was 1.04 ± 0.04 min^{-1}, which was ~2-fold larger than that of heme-WT (0.43 ± 0.01 min^{-1}), suggesting that replacement of His63 with Leu leads to enhancement of heme degradation activity by H_2O_2. Thus, perturbation of hydrogen bonding to heme propionates by replacing His63 with Leu had little effect on the regioselectivity of heme degradation but enhanced H_2O_2-assisted heme-

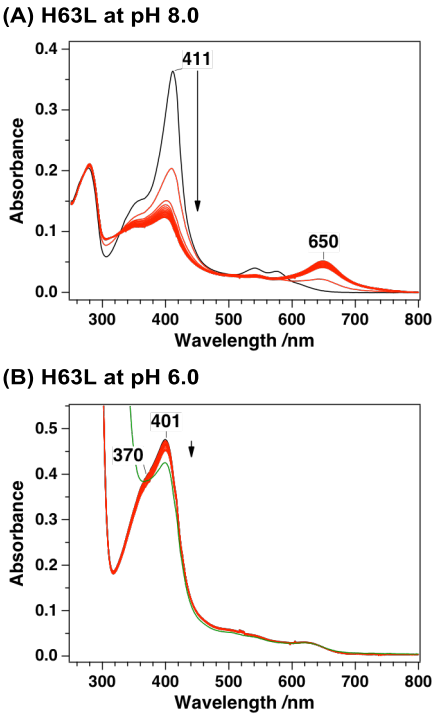


Fig. 4 Heme degradation reactions of heme-H63L HutZ mutants. (A) Reaction of the heme-H63L mutant with H_2O_2. Spectra were measured before and at 1-min intervals for 10 min after the addition of H_2O_2 in 50 mM Tris-HCl and 150 mM NaCl (pH 8.0). (B) Reaction of the heme-H63L mutant with ascorbic acid in the presence of catalase at pH 6.0 (50 mM NaPi and 150 mM NaCl). The final concentration of ascorbic acid was 1 mM. Spectra were measured before the addition of ascorbic acid and at 2-min intervals for 30 min after the addition of ascorbic acid. The black line shows the spectra before addition of H_2O_2 or ascorbic acid, and green line showed the spectra after addition of ferrozine 30 min after initiation of the reaction.

Please do not adjust margins

degrading activity (Fig. 4C). One possibility to explain this finding is that mutation of His63 causes a conformational change to affect accessibility of H_2O_2 to the active site, resulting in enhancement of activity. Accordingly, ligand binding kinetics was investigated.

Cyanide (CN) ion is often used as a probe for assessing accessibility of the ligand-binding site to the heme.[40] The rate of CN binding to heme-HutZ was determined using a stopped-flow apparatus. A typical time trace for the reaction of the heme-H63L mutant with CN at 412 nm is shown in Fig. 5A. Under conditions of excess cyanide, the pseudo-first-order rate constant, k_{obs}, was obtained from a single-exponential fit, which increased linearly with cyanide concentration (Fig. 5B). The slope yielded the second-order rate constant ($k_{on,CN}$). The value for heme-WT HutZ was 0.88 ± 0.01 $mM^{-1}s^{-1}$ while that for the heme-H63L mutant was 0.88 ± 0.02 $mM^{-1}s^{-1}$, indicating that replacement of His63 with Leu does not affect ligand binding properties. The comparable $k_{on,CN}$ values of heme-H63L and heme-WT HutZ indicates that the structure of the heme distal site is not affected by the mutation. This conclusion was supported by resonance Raman spectra of the CO-bound form showing that the frequency of $\nu_{Fe\text{-}CO}$ for the heme-H63L mutant was indistinguishable from that for heme-WT HutZ (Fig. 2C).

Another possible mechanism underlying enhancement of the enzymatic activity of the H63L mutant is a slight difference in heme orientation of the hydroperoxy species (Fe^{3+}-OOH) in the heme binding site. In the heme-WT HutZ complex, heme is cleaved at β- or δ-meso carbon at a ~1:1 ratio,[14] indicating that the terminal OH of the Fe^{3+}-OOH species points toward the β- or δ-meso position of heme. Heme is inserted into the protein along the α-γ axis, which causes β- or δ-selectivity. The direction of the hydroperoxy group is determined by specific amino acid residue(s), such as Arg92 that participates in interactions with iron-bound ligand (Fig. S3†)[17] and thus does not rotate freely. The orientation of Fe^{3+}-OOH in the H63L mutant should be the same as that in heme-WT HutZ, since Arg92 is conserved in this mutant and the frequency and band shape of the Fe-CO stretching mode appears identical to that for heme-WT HutZ (Fig. 2C). Therefore, we propose that a slight in-plane rotation of heme instead of the iron-bound hydroperoxy group in the H63L mutant caused by perturbation of the interactions of heme peripheral groups promotes efficient heme attack by the hydroperoxy group.

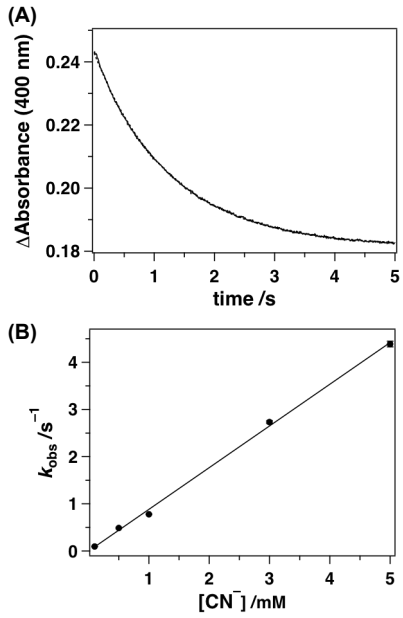


Fig. 5 Cyanide binding to the heme-H63L mutant. (A) Typical time-course of absorbance changes at 400 nm after mixing 5 μM protein with 1 mM cyanide in 50 mM Tris-HCl, 150 mM NaCl, pH 8.0. A line fitted with a single exponential is shown in a broken line. (B) Plots of calculated k_{obs} versus cyanide concentration.

Heme degradation activity of the heme-H63L mutant was further examined using ascorbic acid. At pH 6.0, the Soret band underwent a blue shift to 401 nm with a shoulder at 370 nm (Fig. 4D). During reaction with ascorbic acid, the Soret band diminished gradually. To quantify the amount of Fe^{2+} released from heme by breakage, ferrozine was added to the final reaction solution. Absorbance at 562 nm corresponding to the Fe^{2+}-ferrozine complex did not appear 60 min after the reaction, and the estimated yield of Fe^{2+} released from heme was <5%, indicating that mutation of His63 affects activity at lower pH values.

Heme Binding Ability of the H63L Mutant

Examination of the heme degradation reaction of the heme-H63L mutant at pH 6.0 (Fig. 4D) revealed a distinct absorption spectrum from that of heme-WT HutZ at the same pH, with a blue-shifted Soret band and shoulder at 370 nm,[14] suggesting that affinity for heme is altered by the mutation. Indeed, a heme docking study and mutation experiments proposed that heme is coordinated by His63 and Arg92.[30] For quantitative substantiation of these findings, we obtained apparent dissociation constants ($K_{d,heme}$) of the mutants for heme. Utilizing the differences in Soret bands between free and protein-bound hemin, $K_{d,heme}$ for heme was evaluated (Fig. 6). The titration plot of the H63L mutant for heme at pH 8.0 is presented in Fig. 6A. The $K_{d,heme}$ value was calculated as 0.32 ± 0.06 μM by fitting the plot to Equation 3. This result indicates that mutation of His63 causes only a slight decrease in heme binding affinity, compared with that of WT HutZ (0.052 ± 0.007 μM).[14] The Soret maximum of the heme-H63L mutant at pH 8.0 was 411 nm (Fig. 4A), almost identical to that of WT HutZ (412 nm).[14] In contrast, the Soret band at pH 6.0 shifted to 401 nm with a large shoulder at ~370 nm (Fig. 4B), suggesting that heme was partially released from the protein. At pH 6.0, the plot of the absorption difference at 406 nm revealed a monotonic increase with increasing amounts of heme, characteristic of weak heme binding (Fig. 6B). The exact $K_{d,heme}$ value was not obtained, but estimated as >7 μM. We additionally purified two other His63 mutants, H63G and H63F, for which $K_{d,heme}$ values at pH 8.0 were calculated as 0.049 ± 0.013 and 0.88 ± 0.32 μM, respectively (Fig. S4†). These results suggest that mutation of His63 larger amino acid (Leu or Phe) leads to significant loss of heme binding ability. Contrary to the previous report,[30] our results indicated that His63 is not a

 This journal is © The Royal Society of Chemistry 20xx

Please do not adjust margins

Please do not adjust margins

heme ligand, but contributes to stabilize heme binding, as Asp132.[31]

Role of His63 in Heme binding and Heme Degradation

As described above, perturbation of the putative hydrogen bond between His63 and heme propionate by introducing Leu at this position reduced the heme affinity of HutZ by ~6-fold at pH 8.0. In myoglobin, Arg45 is part of a hydrogen bonding network that includes His64, heme propionates, and water molecules.[41] Mutation of Arg45 enhances the heme dissociation rate by ~10^3-fold, suggesting that Arg45 is a significant regulatory factor in stability of heme binding.[42,43] The effect of mutation of His63 in HutZ on heme affinity was considerably more modest than that of myoglobin mutants, implying that interactions between the residue at this position and propionate are not important for binding of heme to HutZ at pH 8.0.

Reaction of heme-HutZ with H_2O_2 produces a stable intermediate, verdoheme.[14] The peak position of the characteristic band in the visible region for the verdoheme-H63L mutant was 650 nm (Fig. 4C), which was red-shifted by 6 nm from that of WT HutZ.[14] The maximum peak for WT HutZ was far from that of β- or δ-verdoheme reconstituted HO,[39,44] which appeared at 667–668 and 663–664 nm, respectively.[39,44] Upon reduction of the 644 nm species of WT HutZ with ascorbic acid, the band shifted to 671 nm,[45] which was almost identical to that reported for β- or δ-verdoheme-reconstituted HO. This finding indicates that verdoheme observed in the reaction of heme-HutZ with H_2O_2 is Fe^{3+}-verdoheme[45] and not Fe^{2+}-verdoheme, as observed for canonical HOs.[46] In the case of HutZ, Fe^{3+}-verdoheme is preferably formed due to strong electron donation from the heme axial ligand.[45] The red shift of this band for the heme-H63L mutant implies that verdoheme is a mixture of Fe^{3+} and Fe^{2+} species. The increase in Fe^{2+}-verdoheme content signifies a decrease in electron donation from the axial ligand upon mutation of His63. The absorption spectrum of the heme-H63L mutant at pH 6.0 supports less electron donation by the His63 mutant owing to an increase in non-specific heme binding with the Soret band at 370 nm (Fig. 4B). Strong electron donation from proximal His to the heme iron is one of the characteristics of HutZ.[14,45] Interestingly, mutation of His63 led to a decrease in such electron donation (Figs. 4B, 6B).

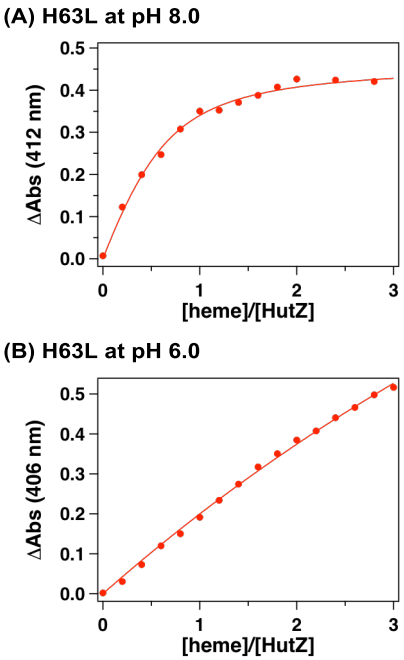


Fig. 6 Heme titration plots of H63L mutant HutZ. Heme binding curve generated from the difference absorbance of the Soret maximum by plotting ΔA_{Soret} vs. molar ratios of heme to protein, specifically, H63L at pH 8.0 (50 mM Tris-HCl, 150 mM NaCl) (A) and 6.0 (50 mM NaPi, 150 mM NaCl) (B). Lines fitted to Equation 3 are shown in solid lines. The protein concentration was 10 μM.

Modulation of Subunit-Subunit Interactions

The absorption maxima of verdoheme at pH 8.0 and ferric heme at pH 6.0 were affected by mutation of His63 (Fig. 4). Similar spectral changes were previously observed for the Glu mutant of Asp132 (D132E) in which the proximal hydrogen bond partner to the heme axial ligand was replaced.[31] In the heme-D132E mutant, the Soret band in the ferric form at pH 6.0 shifted to 403 nm with a large shoulder at 370 nm. The peak of verdoheme at pH 8.0 was additionally shifted from 644 to 652 nm.[31] One prominent feature of the proximal hydrogen bond between Asp132 and His170 of HutZ is that Asp132 is located in a different protomer to His170 (Fig. 7). Thus, the strength of the proximal hydrogen bond in HutZ is related to intersubunit interactions. In fact, introduction of a bulky residue at the subunit-subunit interface leads to alteration of the strength of the proximal hydrogen bond.[47] The resemblance of the absorption spectrum of the heme-H63L mutant at pH 6.0 to that of the heme-D132E mutant indicates that His63 is involved in the pathway of transduction of conformational changes from the distal to proximal heme binding site via Ala31, since His63 and Asp132 exist in the different subunits containing His170 (Fig. 7).

In a previous study, we demonstrated that the distance between His170 and Trp109 in a different subunit containing

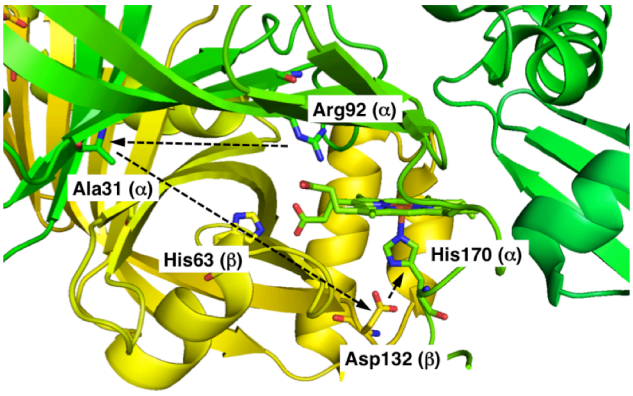


Fig. 7 Putative conformational changes in the transduction pathway. Crystal structure of HugZ from *Helicobacter pylori* (PDB ID code 3GAS). Residues involved in communication between heme distal and proximal sites are highlighted. Amino acid residues are numbered according to the sequence of HutZ from *V. cholerae*. α and β indicate the subunits.

Please do not adjust margins

Please do not adjust margins

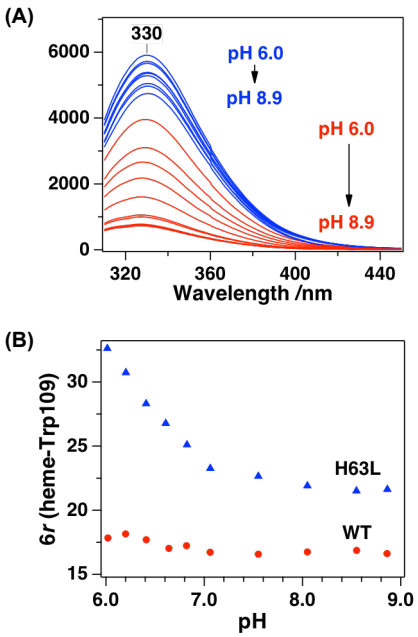


Fig. 8 Fluorescence spectra of the heme-H63L HutZ mutants. (A) Fluorescence spectra of the H63L mutant in the absence and presence of heme. Spectra were recorded with excitation at 295 nm at pH 6.0, 6.2, 6.4, 6.6, 6.8, 7.1, 7.6, 8.1, 8.5 and 8.9. The sample concentration was 3 μM. (B) pH dependence of the distance between heme and Trp109 estimated on the basis of this value of energy transfer efficiency and the Förster distance using equation 2.

His170 depends on pH and is correlated with heme degradation activity.[47] To monitor the changes in subunit-subunit interactions in the H63L mutant, we measured the fluorescence spectra of tryptophan. HutZ possesses a sole tryptophan at position 109 (Fig. S5†). Fluorescence of Trp109 is quenched by heme through energy transfer, and the efficiency is related to the distance between heme and Trp109. Using the fluorescence intensity at 330 nm of apo- and heme-HutZ, we calculated the energy transfer efficiency, *E*, and distance on the basis of Equations 2 and 3, respectively. For heme-WT HutZ, the distance was estimated as 16–17 Å.[47] In contrast, for the H63L mutant, fluorescence of the heme-bound form was significantly increased (Fig. 8B), corresponding to an estimated distance of 22–32 Å (Fig. 8C), clearly indicating that substitution of His63 leads to elongation of the distance, and consequently, lower heme affinity of the H63L mutant.

Conclusions

In summary, this study investigated the potential role of hydrogen bonding between heme 7-propionate and His63 in heme degradation activity. Perturbation of the hydrogen bond as a result of replacing His63 with Leu did not affect the regioselectivity of heme cleavage but slightly increased reactivity to H_2O_2. This result may be due to a slight orientation change of heme within the protein, which triggers the OH group of the Fe^{3+}-OOH species to attack the meso carbon of the porphyrin macrocycle. Additionally, the heme affinity of the H63L mutant was decreased at pH 6.0, probably due to alterations in subunit-subunit interactions. Based on the collective findings, we propose that His63 is involved in subunit-subunit interactions, which may be a contributory factor in the control of heme degradation activity.

Conflicts of interest

There are no conflicts to declare".

Acknowledgements

The authors thank Yuina Nakamura (Hokkaido University) for heme titration experiments. This study was supported in part by Grants-in-Aid for Scientific Research (16K05835 to T.U., and 15H00909 to K.I.) from the Ministry of Culture, Education, Sports, Science, and Technology (MEXT) of Japan.

Notes and references

1 V. Braun and H. Killmann, *Trends Biochem. Sci.*, 1999, **24**, 104–109.
2 S. C. Andrews, A. K. Robinson and F. Rodríguez-Quiñones, *FEMS Microbiol. Rev.*, 2003, **27**, 215–237.
3 M. Miethke and M. A. Marahiel, *Microbiol. Mol. Biol. Rev.*, 2007, **71**, 413–451.
4 R. C. Hider and X. Kong, *Nat. Prod. Rep.*, 2010, **27**, 637–657.
5 M. P. Soares and G. Weiss, *EMBO Rep.*, 2015, **16**, 1482–1500.
6 C. Wandersman and P. Delepelaire, *Annu. Rev. Microbiol.*, 2004, **58**, 611–647.
7 L. L. Anzaldi and E. P. Skaar, *Infect. Immun.*, 2010, **78**, 4977–4989.
8 C. A. Genco and D. W. Dixon, *Mol. Microbiol.*, 2001, **39**, 1–11.
9 J. F. Heidelberg, J. A. Eisen, W. C. Nelson, R. a Clayton, M. L. Gwinn, R. J. Dodson, D. H. Haft, E. K. Hickey, J. D. Peterson, L. Umayam, S. R. Gill, K. E. Nelson, T. D. Read, H. Tettelin, D. Richardson, M. D. Ermolaeva, J. Vamathevan, S. Bass, H. Qin, I. Dragoi, P. Sellers, L. McDonald, T. Utterback, R. D. Fleishmann, W. C. Nierman, O. White, S. L. Salzberg, H. O. Smith, R. R. Colwell, J. J. Mekalanos, J. C. Venter and C. M. Fraser, *Nature*, 2000, **406**, 477–483.
10 E. E. Wyckoff, A. R. Mey and S. M. Payne, *Biometals*, 2007, **20**, 405–416.
11 A. R. Mey and S. M. Payne, *Mol. Microbiol.*, 2001, **42**, 835–849.
12 T. Uchida, T. Funamizu, M. Ogura and K. Ishimori, *Bull. Chem. Soc. Jpn.*, 2017, **90**, 924–930.
13 Y. Sekine, T. Tanzawa, Y. Tanaka, K. Ishimori and T. Uchida, *Biochemistry*, 2016, **55**, 884–893.
14 T. Uchida, Y. Sekine, T. Matsui, M. Ikeda-Saito and K. Ishimori, *Chem. Commun.*, 2012, **48**, 6741–6743.
15 E. E. Wyckoff, M. Schmitt, A. Wilks and S. M. Payne, *J. Bacteriol.*, 2004, **186**, 4142–4151.

This journal is © The Royal Society of Chemistry 20xx

Please do not adjust margins

Please do not adjust margins

16 M. Noguchi, T. Yoshida and G. Kikuchi, *J. Biochem.*, 1982, **91**, 1479–1483.
17 Y. Hu, F. Jiang, Y. Guo, X. Shen, Y. Zhang, R. Zhang, G. Guo, X. Mao, Q. Zou and D.-C. Wang, *J. Biol. Chem.*, 2011, **286**, 1537–1544.
18 D. J. Schuller, A. Wilks, P. R. Ortiz de Montellano and T. L. Poulos, *Nat. Struct. Biol.*, 1999, **6**, 860–867.
19 M. Sugishima, Y. Omata, Y. Kakuta, H. Sakamoto, M. Noguchi and K. Fukuyama, *FEBS Lett.*, 2000, **471**, 61–66.
20 H. Zhou, C. T. Migita, M. Sato, D. Sun, X. Zhang, M. Ikeda-Saito, H. Fujii and T. Yoshida, *J. Am. Chem. Soc.*, 2000, **122**, 8311–8312.
21 G. A. Caignan, R. Deshmukh, A. Wilks, Y. Zeng, H. wei Huang, P. Moënne-Loccoz, R. A. Bunce, M. A. Eastman and M. Rivera, *J. Am. Chem. Soc.*, 2002, **124**, 14879–14892.
22 H. Fujii, X. Zhang and T. Yoshida, *J. Am. Chem. Soc.*, 2004, **126**, 4466–4467.
23 J. Friedman, L. Lad, H. Y. Li, A. Wilks and T. L. Poulos, *Biochemistry*, 2004, **43**, 5239–5245.
24 M. Ratliff, W. Zhu, R. Deshmukh, A. Wilks and I. Stojiljkovic, *J. Bacteriol.*, 2001, **183**, 6394–6403.
25 M. L. Reniere, G. N. Ukpabi, S. R. Harry, D. F. Stec, R. Krull, D. W. Wright, B. O. Bachmann, M. E. Murphy and E. P. Skaar, *Mol. Microbiol.*, 2010, **75**, 1529–1538.
26 S. Nambu, T. Matsui, C. W. Goulding, S. Takahashi and M. Ikeda-Saito, *J. Biol. Chem.*, 2013, **288**, 10101–10109.
27 L. J. Lojek, A. J. Farrand, J. H. Wisecaver, C. E. Blaby-Haas, B. W. Michel, S. S. Merchant, A. Rokas and E. P. Skaar, *mSphere*, 2017, **2**, e00176-17.
28 A. B. Graves, R. P. Morse, A. Chao, A. Iniguez, C. W. Goulding and M. D. Liptak, *Inorg. Chem.*, 2014, **53**, 5931–5940.
29 A. Chao and C. W. Goulding, *Biochemistry*, 2019, **58**, 489–492.
30 X. Liu, J. Gong, T. Wei, Z. Wang, Q. Du, D. Zhu, Y. Huang, S. Xu and L. Gu, *BMC Struct. Biol.*, 2012, **12**, 23.
31 T. Uchida, N. Dojun, Y. Sekine and K. Ishimori, *Biochemistry*, 2017, **56**, 2723–2734.
32 P. Wu and L. Brand, *Anal. Biochem.*, 1994, **218**, 1–13.
33 J. Wang, L. Lad, T. L. Poulos and P. R. Ortiz de Montellano, *J. Biol. Chem.*, 2005, **280**, 2797–2806.
34 R. M. C. Dawson, D. C. Elliot, W. H. Elliot and K. M. Jones, *Data for Biochemical Research*, Oxford University Press Inc., New York, 1995.
35 S. Hu, T. G. Spiro, I. K. Morris, J. P. Singh and K. M. Smith, *J. Am. Chem. Soc.*, 1993, **115**, 12446–12458.
36 S. Hu, K. M. Smith and T. G. Spiro, *J. Am. Chem. Soc.*, 1996, **118**, 12638–12646.
37 E. S. Peterson, J. M. Friedman, E. Y. T. Chien and S. G. Sligar, *Biochemistry*, 1998, **37**, 12301–12319.
38 T. Kitagawa, in *Biological Applications of Raman Spectroscopy*, ed. T. G. Spiro, John Wiley & Sons, New York, III., 1988, pp. 97–131.
39 H. Sakamoto, Y. Omata, Y. Adachi, G. Palmer and M. Noguchi, *J. Inorg. Biochem.*, 2000, **82**, 113–121.
40 A. Brancaccio, F. Cutruzzolá, C. T. Allocatelli, M. Brunori, S. J. Smerdon, A. J. Wilkinson, Y. Dou, D. Keenan, M. Ikeda-Saito and R. E. Brantley, *J. Biol. Chem.*, 1994, **269**, 13843–13853.
41 T. E. Carver, J. S. Olson, S. J. Smerdon, S. Krzywda, A. J. Wilkinson, Q. H. Gibson, R. S. Blackmore, J. D. Ropp and S. G. Sligar, *Biochemistry*, 1991, **30**, 4697–4705.
42 M. S. Hargrove, E. W. Singleton, M. L. Quillin, L. A. Ortiz, G. N. Phillips, J. S. Olson and A. J. Mathews, *J. Biol. Chem.*, 1994, **269**, 4207–4214.
43 M. S. Hargrove, A. J. Wilkinson and J. S. Olson, *Biochemistry*, 1996, **35**, 11300–11309.
44 X. Zhang, H. Fujii, K. M. Matera, C. T. Migita, D. Sun, M. Sato, M. Ikeda-Saito and T. Yoshida, *Biochemistry*, 2003, **42**, 7418–7426.
45 T. Uchida, Y. Sekine, N. Dojun, A. Lewis-Ballester, I. Ishigami, T. Matsui, S.-R. Yeh and K. Ishimori, *Dalton Trans.*, 2017, **46**, 8104–8109.
46 A. Wilks and P. R. Ortiz de Montellano, *J. Biol. Chem.*, 1993, **268**, 22357–22362.
47 T. Uchida, K. Ota, Y. Sekine, N. Dojun and K. Ishimori, *Dalton Trans.*, 2019, **48**, 3973–3983.

Please do not adjust margins